Nonergodicity of the Nose-Hoover chain thermostat in computationally achievable time

Puneet Kumar Patra
Advanced Technology Development Center, Indian Institute of Technology Kharagpur, West Bengal 721302, India

Baidurya Bhattacharya*
Department of Civil Engineering, Indian Institute of Technology Kharagpur, West Bengal 721302, India

(Received 10 July 2014; revised manuscript received 2 September 2014; published 20 October 2014)

The widely used Nose-Hoover chain (NHC) thermostat in molecular dynamics simulations is generally believed to impart the canonical distribution as well as quasi- (i.e., space-filling) ergodicity on the thermostatted physical system (PS). Working with the standard single harmonic oscillator, we prove analytically that the two-chain Nose-Hoover thermostat with unequal thermostat masses approaches the standard Nose-Hoover dynamics, and hence the PS loses its canonical and quasiergodic nature. We also show through numerical simulations over substantially long times that for certain Poincaré sections, for both the equal and unequal thermostat mass cases, the bivariate distribution function of position and momentum (x, p) and of reservoir degrees of freedom (ξ, η) lose their Gaussian nature. Further, the four-dimensional x-p-ξ-η extended phase space exhibits two holes of nonzero measure. The NHC thermostat therefore does not generate the canonical distribution or preserve quasiergodicity for the PS.

DOI: 10.1103/PhysRevE.90.043304 PACS number(s): 05.10.−a, 05.45.Pq

I. INTRODUCTION

Ergodicity of dynamics is a prerequisite for obtaining statistical-mechanical properties of a system from a single dynamical trajectory, generated, for example, through molecular dynamics simulations [1]. The ergodic hypothesis in this context may be stated as follows: given sufficiently long time, a single phase space trajectory of the system must visit all regions of the accessible phase space with the same relative frequency as in the phase space distribution. For a physical system, S, in equilibrium and in contact with a reservoir at constant temperature, T, the equations of motion must result in a trajectory consistent with the canonical distribution $f(\mathbf{x},\mathbf{p}) \propto \exp[-\beta E(\mathbf{x},\mathbf{p})]$. Here $\beta = (k_B T)^{-1}$, where k_B is the Boltzmann constant, and E is the instantaneous energy of S. In this case, ergodicity can also be interpreted as space-filling dynamics (quasiergodicity). Among the several temperature control algorithms available (velocity rescaling [2–5], deterministic [6–15], and stochastic [16–18]), the deterministic thermostats possess the appeal of having autonomous and time reversible dynamics. However, our current understanding of ergodic characteristics of most deterministic thermostats remains primitive. For example, unlike previously thought, not all two-parameter thermostats are ergodic [19].

Possibly the simplest and the most commonly used deterministic thermostat, the Nose-Hoover (NH) thermostat [7,20], suffers from poor ergodicity in systems with few degrees of freedom [19,21–24] and hence does not achieve canonical distribution in such cases (despite constraining the average temperature to the desired one). If and only if the extended system (physical system + reservoir) is ergodic with respect to the invariant measure of system dynamics, S has a canonical distribution [25,26], with its dynamics being phase-space filling.

Investigation of ergodicity, or lack thereof, of NH dynamics in the literature [21,22,24,27] typically involves the simplest possible prototypical system, the single harmonic oscillator, mainly because this system is difficult to thermalize. The NH equations of motion for the single harmonic oscillator may be written as

$$\dot{x} = p, \quad \dot{p} = -x - \eta p, \quad \dot{\eta} = \frac{1}{Q_\eta}(p^2 - k_B T). \qquad (1)$$

In (1), x and p represent the position and velocity of the oscillator, while η represents the thermostat variable with mass Q_η. The nonergodicity of NH dynamics stems from the periodic dynamics of the thermostat variable [28] and the presence of conserved quantities that cause the energy of the system to be bounded [27].

The nonergodicity of NH dynamics, within the framework of the extended system method, is thought to be resolved by using two or more thermostat variables [1,11,19,27]. Two of the most common approaches have been the Nose-Hoover chain (NHC) method [8], which controls the fluctuation of the reservoir momenta, and the kinetic moments method [11], which controls the higher order moments of velocity. In this work we focus only on the NHC thermostat and show that (1) the NHC dynamics is not ergodic, (2) the physical system does not follow the canonical distribution at every Poincaré section, and (3) when the difference in thermostat masses is large, the dynamics due to the NHC reduces to NH dynamics. We also conjecture how previous studies might have missed these points. We limit the scope of this work to a two-chain NHC thermostat, and, in conformity with the existing literature as detailed above, we apply it to the single harmonic oscillator.

II. NOSE-HOOVER CHAIN THERMOSTAT

In addition to controlling the momenta of the particles like (1), the NHC thermostat controls the fluctuations of the thermostat η by coupling it with a new thermostat

*baidurya@civil.iitkgp.ernet.in

variable [1,8]. Fluctuations of the second thermostat can likewise be controlled with a third and so on, thus forming a chain. In one dimension, the NHC equations of motion for a system of N particles and k thermostats $(\eta_1,\ldots,\eta_k)$ are

$$\dot{x}_i = \frac{p_i}{m_i}, \quad \dot{p}_i = \frac{-\partial V}{\partial q_i} - p_i\frac{\eta_1}{Q_1},$$
$$\dot{\eta}_1 = \left[\sum_{i=1}^{N}\frac{p_i^2}{m_i} - Nk_BT\right] - \eta_1\frac{\eta_2}{Q_2},$$
$$\dot{\eta}_j = \left[\frac{\eta_{j-1}^2}{Q_{j-1}} - k_BT\right] - \eta_j\frac{\eta_{j+1}}{Q_{j+1}},$$
$$\dot{\eta}_k = \left[\frac{\eta_{k-1}^2}{Q_{k-1}} - k_BT\right], \tag{2}$$

where m_i is the mass of the ith particle. Like in (1), the variables Q_i are associated with the mass of the ith reservoir variable. An empirical rule of selecting the thermostat masses is $Q_1 = Nk_BT/\omega^2$ and $Q_{j\neq 1} = k_BT/\omega^2$ [8,29]. The frequency, ω, describes the oscillations of kinetic energy between the system and the reservoirs [30]. A sizable set of approximations has been made in developing this relationship, and a suitable choice is usually problem dependent.

For the single harmonic oscillator, with unit mass and spring constant, and coupled to a two-chain NHC thermostat (η,ξ), the dynamics (2) becomes

$$\dot{x} = p, \quad \dot{p} = -x - \frac{\eta p}{Q_\eta},$$
$$\dot{\eta} = p^2 - k_BT - \frac{\eta\xi}{Q_\xi}, \quad \dot{\xi} = \frac{\eta^2}{Q_\eta} - k_BT. \tag{3}$$

The variables Q_η and Q_ξ are the thermostat masses. If the ergodic property is satisfied in the extended system, then the corresponding phase-space density function can be written as

$$f(x,p,\eta,\xi) = \frac{1}{Z}e^{-\frac{\beta}{2}x^2}e^{-\frac{\beta}{2}p^2}e^{-\frac{\beta}{2Q_\eta}\eta^2}e^{-\frac{\beta}{2Q_\xi}\xi^2}, \tag{4}$$

where Z is the normalizing constant. It is trivial to show that (3) in conjunction with (4) satisfy the steady state extended phase space Liouville's equation. Due to the statistical independence of all the variables in (4), their marginal densities are Gaussian. Further, the conditional density function, $f(x,p|\eta=\eta_0,\xi=\xi_0)$, at fixed values of $\xi=\xi_0$ and $\eta=\eta_0$ is uncorrelated bivariate normal:

$$f(x,p|\eta=\eta_0,\xi=\xi_0) = \frac{1}{Z'}e^{-\beta x^2/2}e^{-\beta p^2/2}. \tag{5}$$

Expression (5) must hold true for all Poincaré sections for the NHC to sample from a canonical distribution, and any deviation of the joint probability distribution function (JPDF) from bivariate Gaussian indicates the noncanonical nature of the dynamics. If such noncanonical dynamics exist, then the overall dynamics must be nonergodic with holes present in the phase space. A similar argument holds true for conditional distribution of $f(\eta,\xi|x=x_0,p=p_0)$ and for the univariate conditional distribution function: $f(x|p=p_0,\eta=\eta_0,\xi=\xi_0)$. All previous attempts at proving that the dynamics due to (3) is ergodic involved showing that the marginal distributions of position (x) and velocity (p) are Gaussian [8,31], and no conclusive proof of its ergodicity has been put forward so far [27].

III. NONERGODICITY OF THE NOSE-HOOVER CHAIN THERMOSTAT WITH TWO CHAINS

We simulated the extended system involving the harmonic oscillator (3) at $\beta=1$ using four thermostat mass pairs: $Q_\eta,Q_\xi = (1,1),(10,0.1),(50,0.02)$, and $(100,0.01)$. Since the fluctuations of reservoir η are controlled by the second reservoir ξ, effective thermostatting of η can occur only if $Q_\xi \ll Q_\eta$. Equations of motion (3) were integrated for 200 billion time steps each of 0.001. Various initial conditions were chosen. The canonical nature of the physical system, or, equivalently, the ergodic nature of the extended system, was investigated on various Poincaré sections of the four-dimensional phase space through joint moments, Kullback-Leibler distance, Hellinger distance, and presence of holes of nonzero measure.

When initial conditions were chosen far from fixed points (given by $x=0,p=0,\eta=\pm\sqrt{Q_\eta},\xi=\mp Q_\xi/\sqrt{Q_\eta}$), the trajectories never came close to the fixed point during the simulation duration. Four such Poincaré sections initialized at $x=1.1,p=1.1,\eta=0,\xi=0$ are shown in Fig. 1. In each case there is a significant deviation from bivariate normal near the origin $(x=0,p=0)$: the JPDF is in fact zero in Figs. 1(a) and 1(c). This deviation would be missed if, instead, the JPDF of x-p is obtained by projecting the dynamics from the four-dimensional space onto the x-p plane. The deviation from Gaussian becomes even more apparent when one studies the Poincaré section defined at $x=0$ and $p=0$. In fact, one can conclude just by looking at the JPDFs of η,ξ (see Fig. 2) that they are not bivariate Gaussian.

We checked the convergence in distribution of the JPDF (f_1) of x,p (5) to the uncorrelated standard bivariate normal (f_2) with the help of Hellinger [32] and symmetrical form of Kullback-Leibler (KL) [33] distances:

$$D_H(f_1||f_2) = \frac{1}{\sqrt{2}}\sqrt{\sum_{i,j}[\sqrt{f_1(i,j)}-\sqrt{f_2(i,j)}]^2}, \tag{6}$$

$$D_{KL}(f_1||f_2) = \sum_{i,j}\left[f_1(i,j)\ln\frac{f_1(i,j)}{f_2(i,j)} + f_2(i,j)\ln\frac{f_2(i,j)}{f_1(i,j)}\right]. \tag{7}$$

The evolution of the Hellinger and KL distances between the uncorrelated standard bivariate normal and the JPDF of (x,p) at each of the Poincaré sections of Fig. 1 is shown in Fig. 3. Despite long simulations, the distributions do not converge (Fig. 3) to the uncorrelated bivariate normal.

We also looked at the first six even joint moments of x,p: $\langle x^{2n}p^{2n}\rangle$ (n varying from one to six) and found that deviations were as high as 43%, 75%, 40%, and 226%, respectively, in the four cases from those of standard uncorrelated bivariate normal. Figure 4 shows the convergence of the fourth and

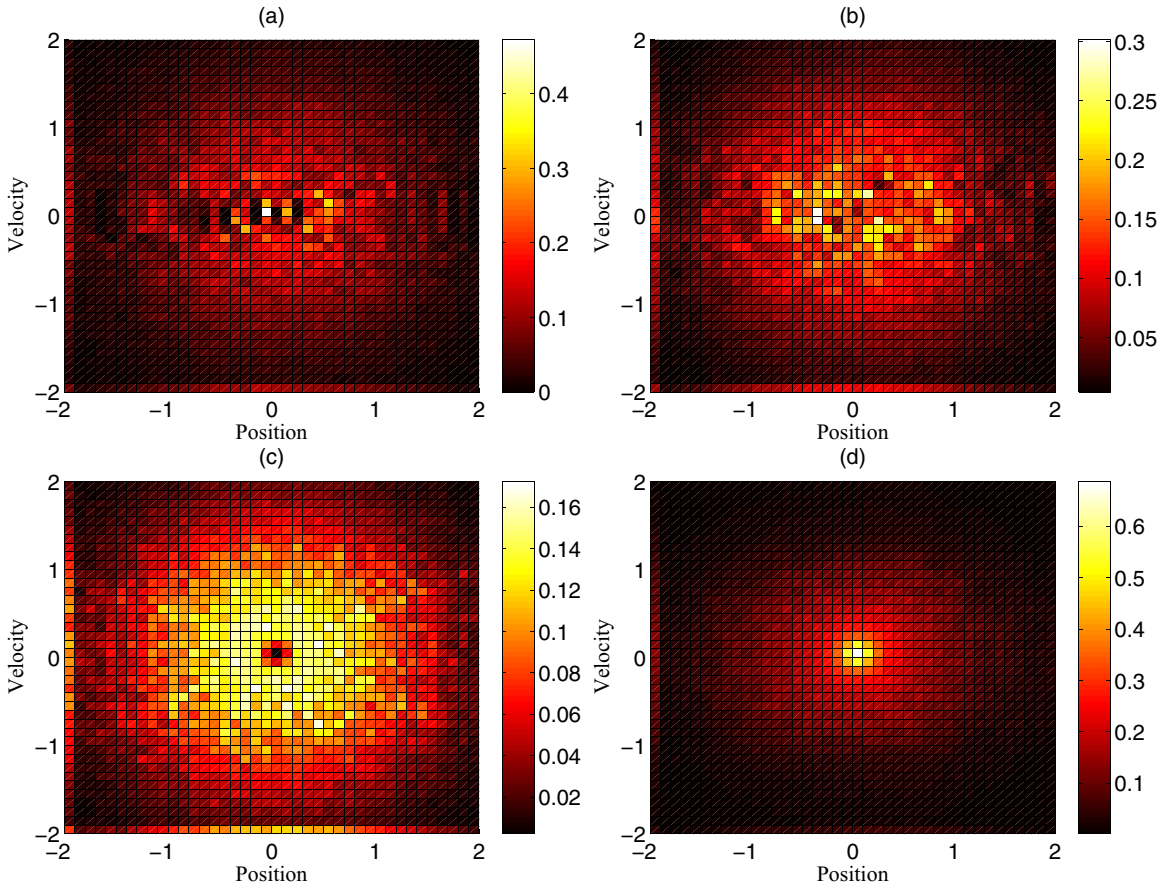

FIG. 1. (Color online) JPDF plot of x-p corresponding to different Poincaré sections for four different pairs of thermostat masses with initial conditions as $x = 1.1, p = 1.1, \eta = 0, \xi = 0$. The different figures correspond to (a) $Q_\eta = 1, Q_\xi = 1$ at the Poincaré section $\eta = -1, \xi = 1$, (b) $Q_\eta = 10, Q_\xi = 0.1$ at the Poincaré section $\eta = -3.16, \xi = 0.03$, (c) $Q_\eta = 50, Q_\xi = 0.02$ at the Poincaré section $\eta = -7.07, \xi = 0.003$, (d) $Q_\eta = 100, Q_\xi = 0.01$ at the Poincaré section $\eta = -10, \xi = -0.003$. For each case we can observe that there is a deviation from normal distribution.

the sixth joint moments for two thermostat mass pairs. It can be clearly seen that the moments have converged to incorrect values.

Previous studies have used marginal distributions as a basis to argue that the NHC generates canonical dynamics. We too found that the non-Gaussian features are overlooked if one looks only at the marginal distributions, or JPDFs obtained through projections on a plane. The long-time averaged temperature, as calculated from the second moment of velocity (using the projected dynamics), is 1.0. So we have a situation where although the system remains at the desired temperature, a correct canonical ensemble is not produced. To illustrate this point, we simulated 10 million values of a four-dimensional (n_1-n_2-n_3-n_4) joint standard normal. A small four-dimensional hole (of radius 0.25) is then embedded by deleting the points that lie within the boundary $n_1^2 + n_2^2 + n_3^2 + n_4^2 = 0.0625$. The projected n_1-n_2 plot and the marginal distributions are shown in Fig. 5. It is interesting to see that there is no deviation from the standard normal distribution. In fact, the first three even marginal and joint moments agree well with the standard normal distribution: $\langle n_1^2 \rangle = 1.000$, $\langle n_1^4 \rangle = 3.000$, $\langle n_1^6 \rangle = 15.007$, $\langle n_2^2 \rangle = 0.999$, $\langle n_2^4 \rangle = 2.999$, $\langle n_2^6 \rangle = 14.992$, $\langle n_1^2 n_2^2 \rangle = 0.999$, $\langle n_1^4 n_2^4 \rangle = 9.003$, and $\langle n_1^6 n_2^6 \rangle = 227.496$. Thus, it becomes evident that analyzing projections for ergodicity washes out the non-Gaussian nature due to the presence of embedded holes.

The nonergodic nature of the dynamics is further revealed by the phase-space plots in Figs. 6 and 7 (corresponding to Figs. 1 and 2, respectively). Holes are clearly present in the phase space. As the difference of the thermostat masses decreases, the holes rotate in the plane. Due to the complexity of the dynamics in four-dimensional space, attempts to find stable periodic orbits were unsuccessful. We therefore take an alternate route to confirm that the holes are of nonzero measure. We focused on one of the possible locations of holes because of antisymmetry of Fig. 7. Instead of working with Poincaré sections, we took a splice of much larger width in x-p. We looked at the region $-\lambda \leqslant x \leqslant \lambda$, $-\lambda \leqslant p \leqslant \lambda$ and kept increasing λ until the η-ξ plot showed no existence of a sparsely populated region. If the unoccupied regions in Figs. 6 and 7 were limited to just one hyperplane, i.e., $\lambda \approx 0$, when sparsely populated regions disappear, then the measure of the holes present in the system would be zero and the dynamics would still be ergodic. The corresponding JPDFs would have been uncorrelated bivariate normal. Figure 8 shows the presence of very small unpopulated regions when $\lambda = 0.1$. This confirms that there is a hole whose x-p boundary is given by $|x| \approx 0.1$ and $|p| \approx 0.1$. Further, unlike other cases, the

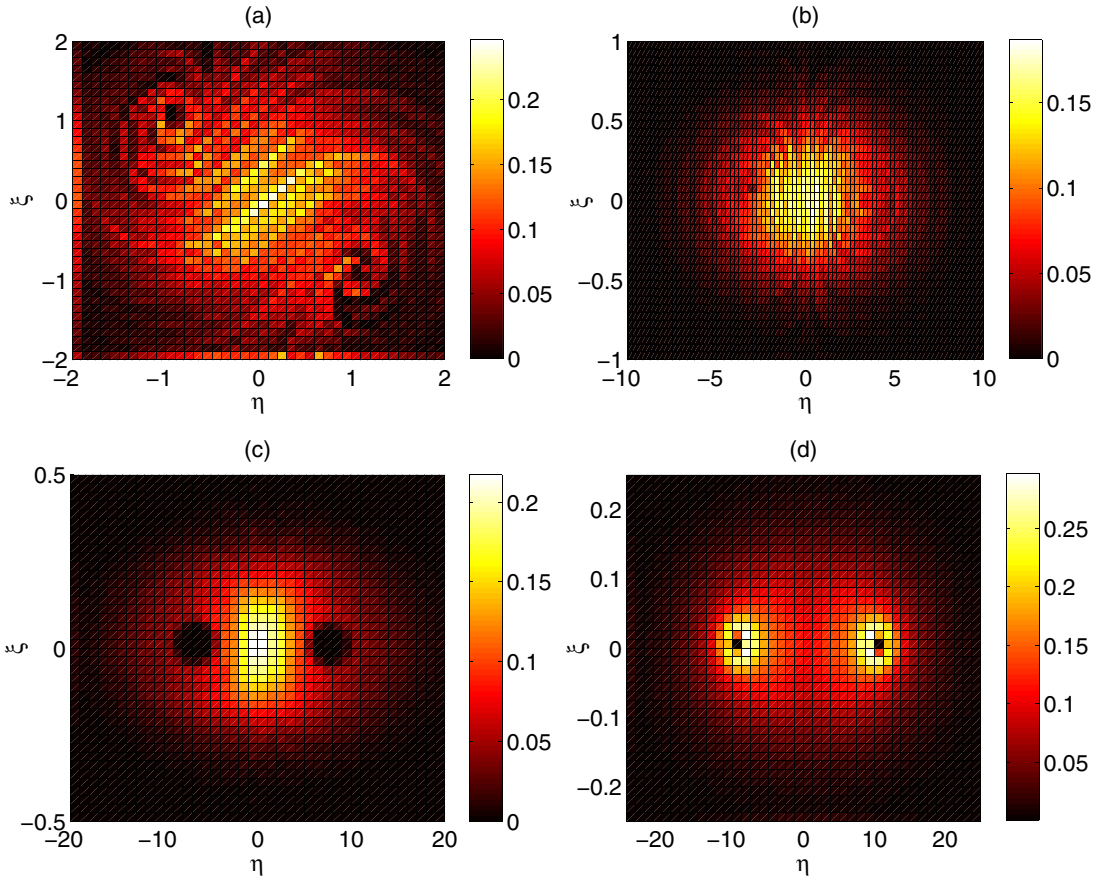

FIG. 2. (Color online) The η-ξ joint probability density plots for a Poincaré section at $x = 0, p = 0$. The different figures correspond to (a) $Q_\eta = 1, Q_\xi = 1$, (b) $Q_\eta = 10, Q_\xi = 0.1$, (c) $Q_\eta = 50, Q_\xi = 0.02$, (d) $Q_\eta = 100, Q_\xi = 0.01$. The initial conditions remain the same as before. The figures indicate the presence of two holes in the system dynamics.

hole for the case of $Q_\eta = 100, Q_\xi = 0.01$ was found to be a through hole. The size of the hole progressively decreases and reaches a minimum value when both thermostat masses are set at 1 (but does not remain confined to one hyperplane and hence is of nonzero measure).

Theoretically, it is possible to understand why the NHC shows end-to-end holes for a large difference in masses. Using the transformation $\eta' = \eta/Q_\eta$ and $\xi' = \xi/Q_\xi$, (3) can be written in terms of η' and ξ'. Choosing $x = r\sin\theta$ and $p = r\cos\theta$, and rearranging in terms of $\dot{r}$ and $\dot{\theta}$, (3) can be

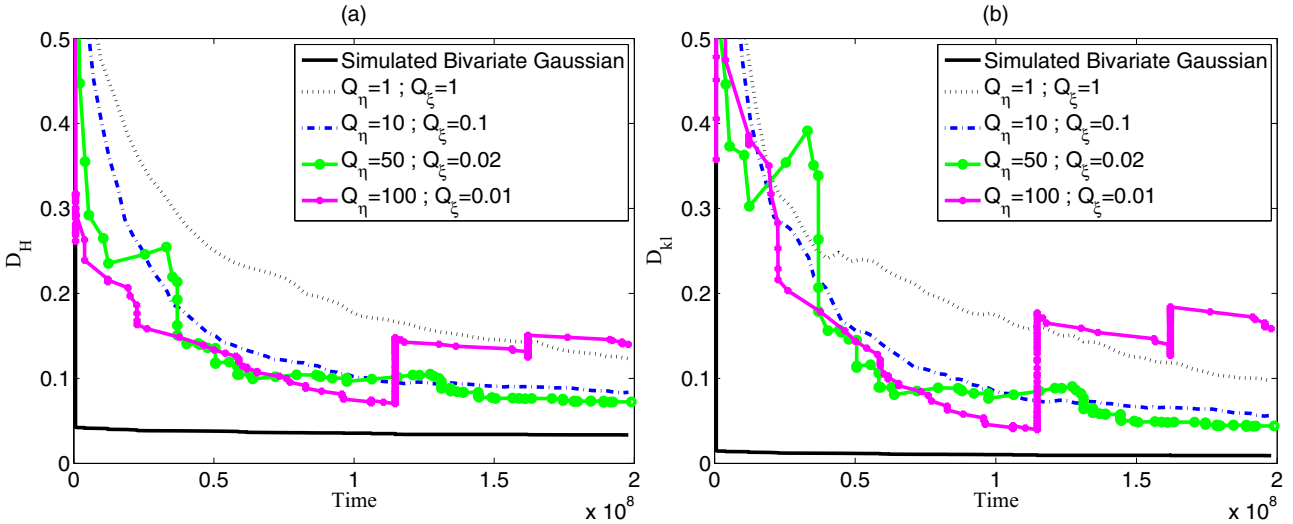

FIG. 3. (Color online) Convergence of Hellinger (a) and modified KL distances (b) for various cases. Bins of size $\Delta x = 0.1$ and $\Delta p = 0.1$ are used. None of the distributions converge to the standard uncorrelated bivariate normal.

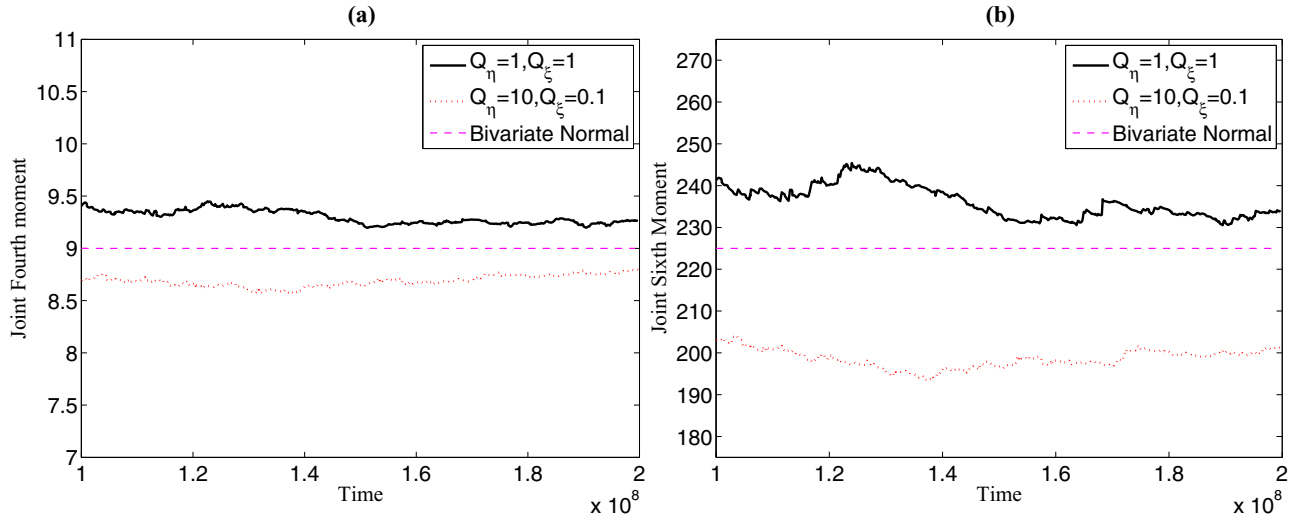

FIG. 4. (Color online) Convergence of the (a) joint fourth moment and (b) joint sixth moment of position and velocity for two values of thermostat parameters. It is evident that the moments have converged to values that deviate from the desired standard normal values (shown as dashed pink line). A similar behavior was observed for other moments as well.

rewritten as

$$\dot{r} = -\eta' r\cos^2\theta, \quad \dot{\theta} = 1 + \eta'\sin\theta\cos\theta,$$
$$\dot{\eta}' = \frac{1}{Q_\eta}(r^2\cos^2\theta - k_BT) - \eta'\xi', \quad \dot{\xi}' = \frac{\eta'^2 Q_\eta}{Q_\xi} - \frac{k_BT}{Q_\xi}. \tag{8}$$

Under the scenario $Q_\xi \ll Q_\eta$, the fluctuations of ξ' occur at a much faster rate than other variables. As a result, ξ' may be replaced by its average. Once the steady state is reached, ξ' fluctuates around the mean, and consequently its average is zero. Therefore, (8) can effectively be written in terms of three variables:

$$\dot{r} = \eta' r\cos^2\theta, \quad \dot{\theta} = 1 + \eta'\sin\theta\cos\theta,$$
$$\dot{\eta}' = \frac{(r^2\cos^2\theta - k_BT)}{Q_\eta}. \tag{9}$$

Expressions (9) are the same as the standard NH dynamics [27] and hence show similar features (as well as problems) as the NH thermostat.

IV. CONCLUSIONS

To summarize, we used numerical simulations to demonstrate that in the rather long-time duration considered, the Nose-Hoover chain thermostat is unable to generate a canonical distribution in certain Poincaré sections, despite the overall projection being deceptively close to canonical. This occurs due to the presence of two four-dimensional holes of nonzero measure. We have utilized the extended-phase space distribution due to the NHC thermostat along with the independence of the variables involved to argue that a correct ergodic dynamics implies validity of (5) at every Poincaré section. Deviation of (5) from an uncorrelated bivariate normal

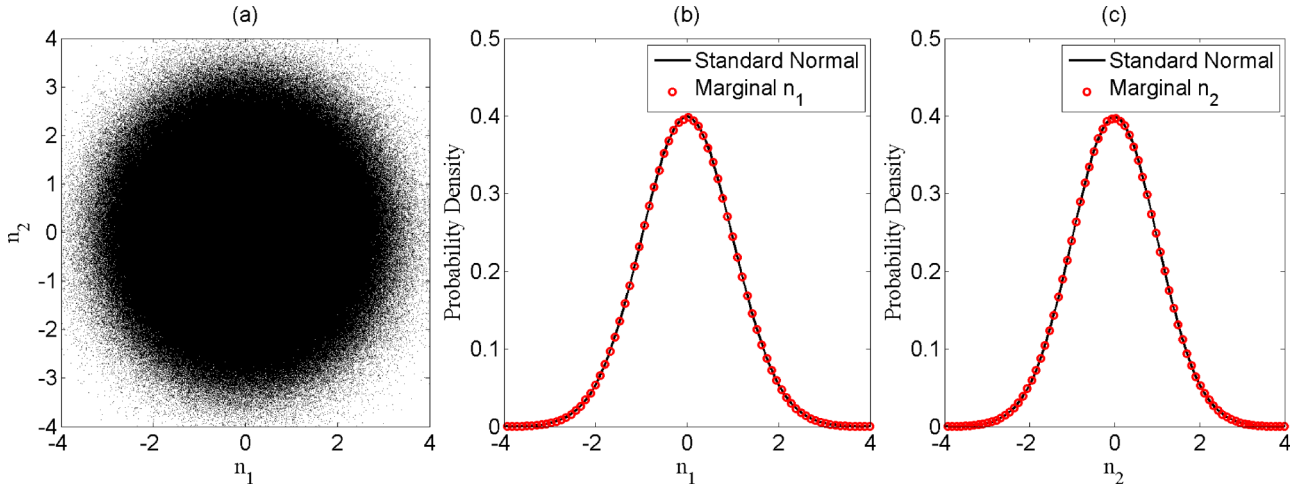

FIG. 5. (Color online) Inability of projected variables n_1-n_2 to capture the four-dimensional hole of radius 0.25 forcefully embedded within a four-dimensional joint standard normal. (a) Projected values of n_1-n_2 onto the $n_3 = 0, n_4 = 0$ plane. (b) Marginal distribution of n_1 and (c) marginal distribution of n_2. No difference in marginal distributions from that of standard normal can be observed.

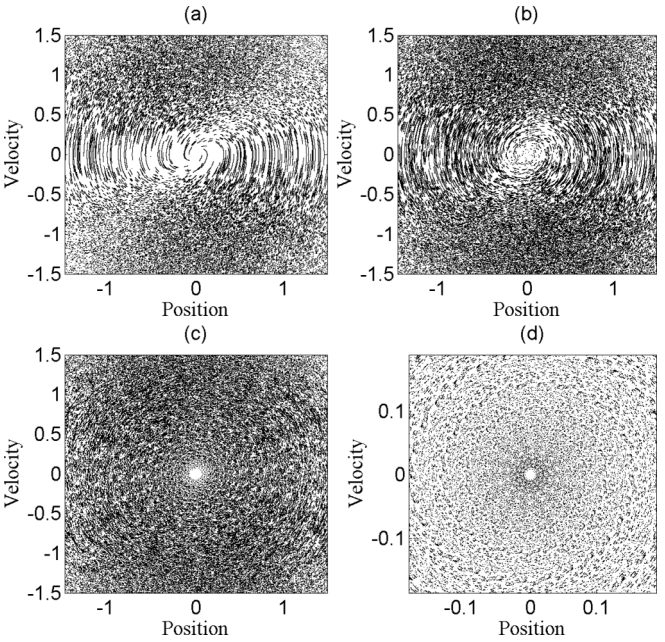

FIG. 6. Phase space plot of x-p corresponding to different Poincaré sections for four different pairs of thermostat masses. The different figures correspond to (a) $Q_\eta = 1, Q_\xi = 1$ at the Poincaré section $\eta = -1, \xi = 1$, (b) $Q_\eta = 10, Q_\xi = 0.1$ at the Poincaré section $\eta = -3.16, \xi = 0.03$, (c) $Q_\eta = 50, Q_\xi = 0.02$ at the Poincaré section $\eta = -7.07, \xi = 0.003$, (d) $Q_\eta = 100, Q_\xi = 0.01$ at the Poincaré section $\eta = -10, \xi = -0.003$. Existence of unoccupied regions near origin for all the cases suggests that holes are present in phase space.

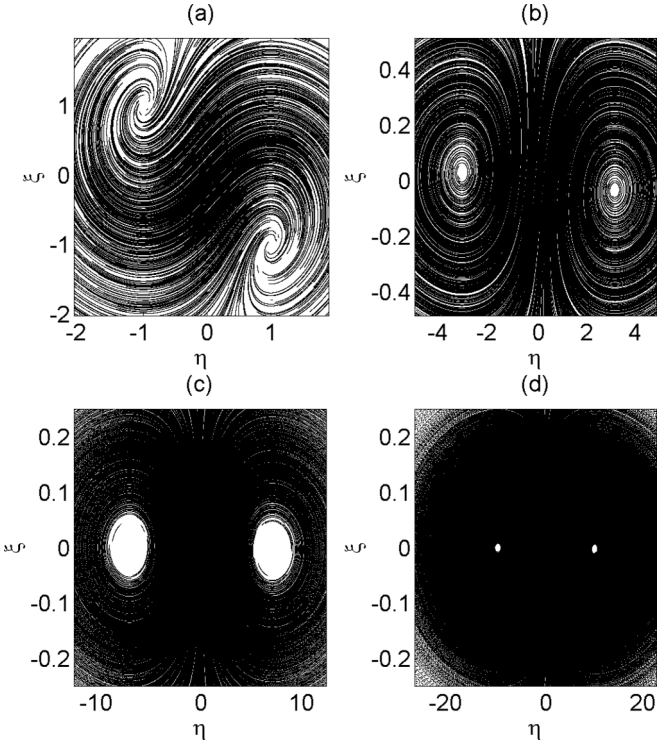

FIG. 7. Phase space plot of η-ξ corresponding to different Poincaré sections for four different pairs of thermostat masses. The different figures correspond to (a) $Q_\eta = 1, Q_\xi = 1$, (b) $Q_\eta = 10, Q_\xi = 0.1$, (c) $Q_\eta = 50, Q_\xi = 0.02$, (d) $Q_\eta = 100, Q_\xi = 0.01$. Two holes can be easily seen.

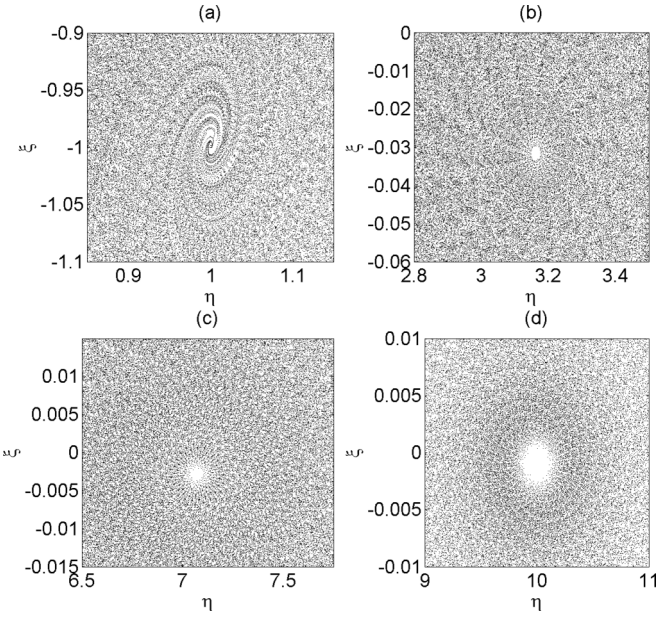

FIG. 8. Nonzero measure holes in each of the four cases using 20 billion time steps each of 0.01. In each of the figures, $-0.1 \leqslant x \leqslant 0.1, -0.1 \leqslant p \leqslant 0.1$. The different figures correspond to (a) $Q_\eta = 1, Q_\xi = 1$, (b) $Q_\eta = 10, Q_\xi = 0.1$, (c) $Q_\eta = 50, Q_\xi = 0.02$, (d) $Q_\eta = 100, Q_\xi = 0.01$.

distribution is an indicator of nonergodicity of the dynamics. Merely showing the Gaussian nature of marginal distributions of position and velocity, as has been done in the past, is not sufficient to prove ergodicity.

We observed significant deviation of the JPDFs from a bivariate uncorrelated normal distribution. The deviations were quantified by analyzing the first six even joint moments of position and velocity. The deviations are much higher for unequal thermostat masses than the equal thermostat mass case. To check the convergence in distribution of the JPDFs, we used two functions: Kullback-Leibler divergence and Hellinger distance, each suggesting that the distributions do not converge to a bivariate normal. However, due to the complexity of the dynamics in the four-dimensional space, attempts to find stable periodic orbits were unsuccessful.

Since the trajectories of x, p, η, and ξ each constitutes a stochastic process, it can also be argued that the EOMs (3) do not support the assumption of ergodicity (4), which implies each of the four processes is stationary Gaussian. For if p is a Gaussian process, so is its derivative $\dot{p}$, and if p is stationary Gaussian, it is also independent of $\dot{p}$ at the same instant, both of which are violated by (3) (and likewise for η and ξ). However, we do not probe this stochastic process angle further in this paper.

ACKNOWLEDGMENTS

We wish to thank Prof. William G. Hoover for his several useful comments that helped in improving the quality of this document.

[1] W. G. Hoover and O. Kum, Phys. Rev. E **56**, 5517 (1997).
[2] L. V. Woodcock, Chem. Phys. Lett. **10**, 257 (1971).
[3] W. G. Hoover, A. J. C. Ladd, and B. Moran, Phys. Rev. Lett. **48**, 1818 (1982).
[4] D. J. Evans, J. Chem. Phys. **78**, 3297 (1983).
[5] D. J. Evans, W. G. Hoover, B. H. Failor, B. Moran, and A. J. C. Ladd, Phys. Rev. A **28**, 1016 (1983).
[6] S. Nose, J. Chem. Phys. **81**, 511 (1984).
[7] W. G. Hoover, Phys. Rev. A **31**, 1695 (1985).
[8] G. J. Martyna, M. L. Klein, and M. Tuckerman, J. Chem. Phys. **97**, 2635 (1992).
[9] I. P. Hamilton, Phys. Rev. A **42**, 7467 (1990).
[10] R. G. Winkler, Phys. Rev. A **45**, 2250 (1992).
[11] W. G. Hoover and B. L. Holian, Phys. Lett. A **211**, 253 (1996).
[12] S. D. Bond, B. J. Leimkuhler, and B. B. Laird, J. Comput. Phys. **151**, 114 (1999).
[13] C. Braga and K. P. Travis, J. Chem. Phys. **123**, 134101 (2005).
[14] A. Samoletov, C. Dettmann, and M. Chaplain, J. Stat. Phys. **128**, 1321 (2007).
[15] P. K. Patra and B. Bhattacharya, J. Chem. Phys. **140**, 064106 (2014).
[16] H. C. Andersen, J. Chem. Phys. **72**, 2384 (1980).
[17] G. S. Grest and K. Kremer, Phys. Rev. A **33**, 3628 (1986).
[18] T. Schneider and E. Stoll, Phys. Rev. B **17**, 1302 (1978).
[19] J. C. Sprott, W. G. Hoover, and C. G. Hoover, Phys. Rev. E **89**, 042914 (2014).
[20] W. G. Hoover, *Computational Statistical Mechanics* (Elsevier, Amsterdam, 1991).
[21] F. Legoll, M. Luskin, and R. Moeckel, Arch. Ration. Mech. Anal. **184**, 449 (2007).
[22] D. Kusnezov, A. Bulgac, and W. Bauer, Ann. Phys. **204**, 155 (1990).
[23] A. Bulgac and D. Kusnezov, Phys. Rev. A **42**, 5045 (1990).
[24] H. A. Posch, W. G. Hoover, and F. J. Vesely, Phys. Rev. A **33**, 4253 (1986).
[25] K. Cho and J. D. Joannopoulos, Phys. Rev. A **45**, 7089 (1992).
[26] S. Nose, Prog. Theor. Phys. Suppl. **103**, 1 (1991).
[27] H. Watanabe and H. Kobayashi, Phys. Rev. E **75**, 040102 (2007).
[28] H. Watanabe and H. Kobayashi, Mol. Simul. **33**, 77 (2007).
[29] D. J. Tobias, G. J. Martyna, and M. L. Klein, J. Phys. Chem. **97**, 12959 (1993).
[30] J. E. Basconi and M. R. Shirts, J. Chem. Theory Comput. **9**, 2887 (2013).
[31] M. E. Tuckerman and G. J. Martyna, J. Phys. Chem. B **104**, 159 (2000).
[32] L. M. Yang, Grace Lo, and Le Cam, *Asymptotics in Statistics: Some Basic Concepts* (Springer, Berlin, 2000).
[33] S. Kullback and R. A. Leibler, Ann. Math. Stat. **22**, 79 (1951).